African Hot Spot Volcanism: Small-Scale Convection in the Upper Mantle Beneath Cratons

Scott D. King [1]* and Jeroen Ritsema [2]

Numerical models demonstrate that small-scale convection develops in the upper mantle beneath the transition of thick cratonic lithosphere and thin oceanic lithosphere. These models explain the location and geochemical characteristics of intraplate volcanos on the African and South American plates. They also explain the presence of relatively high seismic shear wave velocities (cold downwellings) in the mantle transition zone beneath the western margin of African cratons and the eastern margin of South American cratons. Small-scale, edge-driven convection is an alternative to plumes for explaining intraplate African and South American hot spot volcanism, and small-scale convection is consistent with mantle downwellings beneath the African and South American lithosphere.

Cratons are regions of continents that have not been affected by tectonic processes for more than one billion years. Relatively low surface heat flow (*1*), diamond inclusions in kimberlites (*2*), and a relatively cold and thick keel (*3*) with high seismic velocities to about 250 km depth (*4*) distinguish cratons from other continental lithosphere. Although cratons are commonly envisioned as stable regions of Earth's lithosphere, the change in lithospheric thickness and, hence, the relatively strong lateral temperature and viscosity contrasts at the edges of cratons induce a small-scale form of convective flow in the mantle beneath the craton margin. Numerical (*5*) and laboratory (*6*) investigations indicate that such convective flow, commonly termed edge-driven convection, consists of downwellings extending as deep as the mantle transition zone (about 660 km) beneath the margins of cratons and upwellings at about 500 to 1000 km distance from the margins of cratons. Previous workers have suggested that edge-driven convection may be responsible for the formation of the Bermuda Rise (*7*), the North Atlantic Tertiary Volcanics (*8*), and flood basalt magmatism at the peripheries of cratonic provinces (*9*). Here, we suggest that intraplate volcanos (hotspots) on the African and South American plates (Fig. 1) are linked to edge-driven convection on the basis of numerical simulations of mantle flow and images of seismic velocity anomalies in the African upper mantle.

Our model of edge-driven convection is based on the temperature and velocity fields, computed using a compressible convection formulation for a two-dimensional Cartesian geometry (Fig. 2) (*10*). The initial thermal structure of an ocean basin is calculated using the solution for a moving plate, whereas the thermal structure of the cratonic lithosphere is calculated using the half-space solution and assuming that the

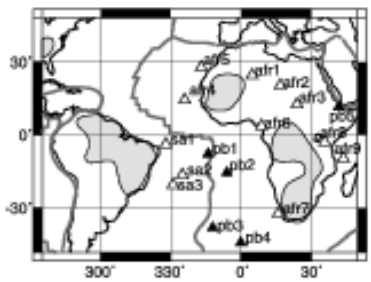

Fig. 1. Location of hot spots (triangles), cratons (gray shading), and plate boundaries (gray line). The boundaries of cratons are defined seismically: they circumscribe regions of S20RTS at 100 km depth where the shear wave velocity perturbation from the PREM model is 4% or larger. The hotpots are taken from the list compiled by Sleep (*20*). The intraplate "African hot spots" are denoted by white triangles (afr1, Ahaggar; afr2, Tibesti; afr3, Jebel Mara; afr4, Cape Verde; afr5, Canary; afr6, Mt Cameroon; afr7, Verna; afr8, Victoria; and afr9, Comores), as are the "South American" hotspots (sa1, Fernando; sa2, Arnold; and sa3, Trindad). "Plate Boundary" hot spots are denoted with black triangles (pb1, Ascension; pb2, St. Helena; pb3, Tristan da Cunha; pb4, Discovery; and pb5, Afar).

[1]Department of Earth and Atmospheric Sciences, Purdue University, West Lafayette, IN 47907–1397, USA. [2]Seismological Laboratory, California Institute of Technology, Pasadena, CA 91125, USA.

*To whom correspondence should be addressed. E-mail: sking@purdue.edu

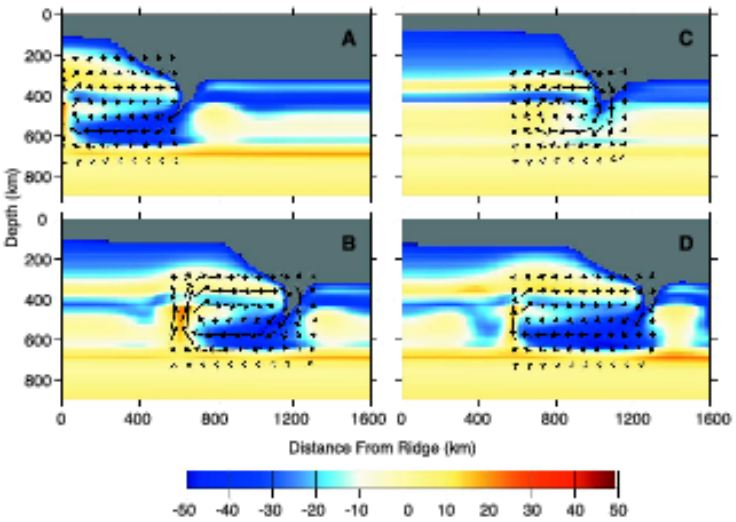

Fig. 2. The temperature anomalies (adiabatic temperature profile removed) and velocity fields from calculations with a step change in lithospheric thickness. The width of the ocean basin (thin lithosphere) is 600 (A) and 1900 km (B). In each calculation, the width of the ocean basin is fixed throughout time. Both panels are taken 50 My after the initial condition. The temporal evolution of the calculation in panel (B) is shown in (C) and (D) at 20 My and 100 My after the initial condition, respectively. The parameters used in these calculations are described in the text and notes. Because of the symmetry of the boundary conditions, only the left half of the ocean basin is shown; the solution can be reflected about the left edge of the model. Because the flow is confined to the upper mantle, only a subregion of the the calculation is shown; the width and depth of the calculation extend to 2890 km.

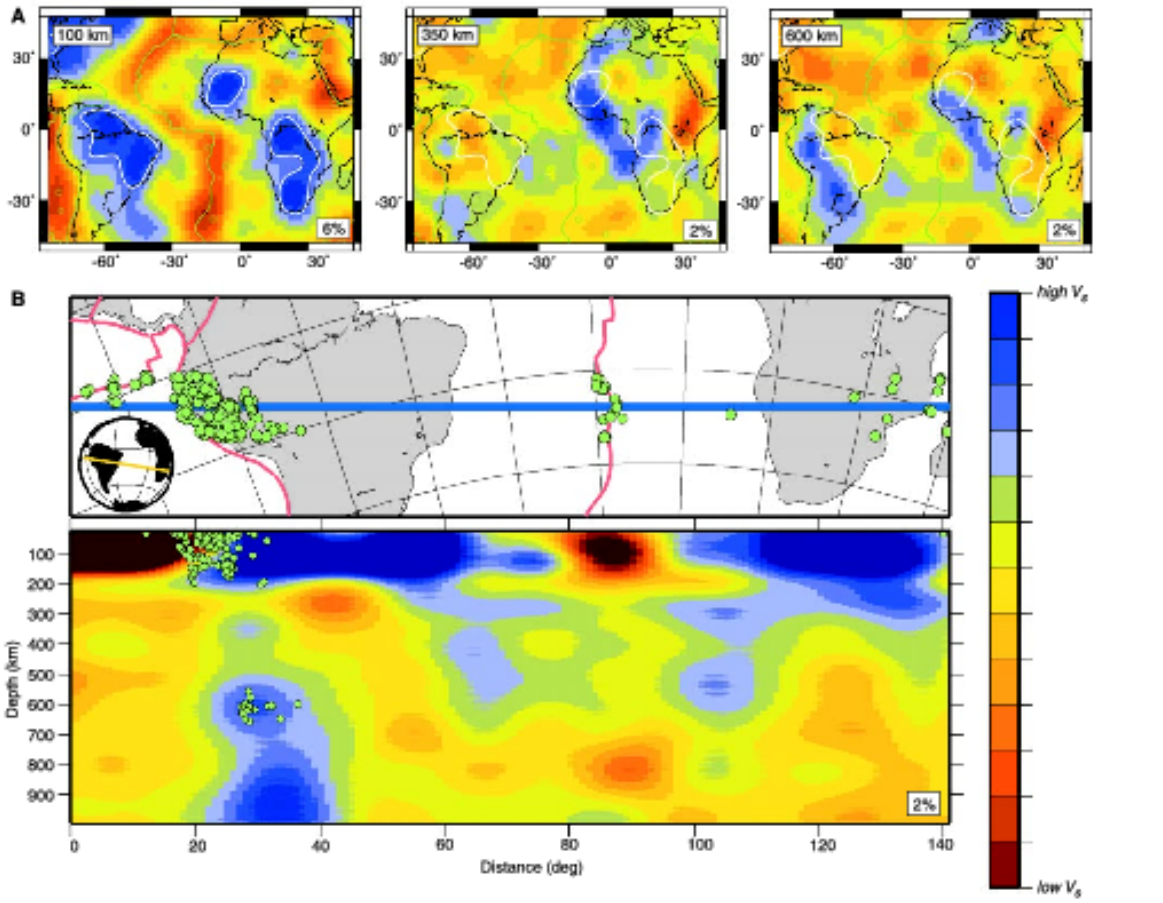

Fig. 3. (A) Horizontal cross sections through S20RTS at at depths of 100, 350, and 600 km. Relative high- and low-velocity regions are indicated by blue and red, respectively, with an intensity that is proportional to the amplitude of the velocity perturbation from the PREM. Green lines represent plate boundaries. White lines circument regions in the mantle where the seismic velocity at a depth of 100 km is larger than in the PREM by 4% or more. These regions roughly outline the location of Precambrian cratons. (B) A 140°-wide cross section through S20RTS across South America and southern Africa. The green circles indicate locations of earthquakes in the Harvard Centroid Moment Tensor catalog.

craton is uniformly 500 million years (My) old (*11*). The model also contains solid-solid phase transformations at 410 and 660 km depth (*12*), which confine edge-driven convection to the upper mantle (*13*). The viscosity of the fluid depends on pressure and temperature, following the creep properties of olivine (*14*). The location of the craton with respect to the edges of the computational domain is fixed in each calculation. The distance between the edge of the craton and the ocean ridge is varied from 400 to 1600 km in a series of calculations to study the pattern of the small-scale flow as the width of the ocean basin is increased.

When the ocean basin is narrow (Fig. 2A), an upwelling forms along the edge of the computational domain, which represents the central spreading axis of the ocean basin. A downwelling forms beneath the craton, slightly on the craton side of the craton-ocean margin. As the width of the ocean basin increases with time (Fig. 2B), the upwelling moves off the spreading axis while the downwelling remains fixed with respect to the craton-ocean boundary. The resulting edge-driven convection cell is, at most, 800 to 1000 km wide regardless of the location of the craton. Edge-driven convection reaches a peak velocity of about 30 mm/year at an elapsed time of about 80 to 100 My. After 100 My, the vigor of the flow slowly decreases. The cratonic root in our model is cold and hence more viscous than the surrounding mantle. This is sufficient to stablize a cratonic root for up to a billion years (*15*). We infer that the intraplate African and South American hotspots (denoted by white triangles in Fig. 1), which are located 600 to 1000 km from the margins of the African and South American cratons, are the surface manifestation of the upwelling flow seen in the edge-driven convection model (Fig. 2), and not deep mantle plumes. Because Africa is thought to have remained nearly stationary with respect to the deep mantle (*16*), edge-driven convection may be easier to detect under African than at moving cratons, where the plate-scale flow could significantly alter the pattern of edge-driven flow.

Although previous studies of edge-driven convection have focused on the hot, upwelling flow, downwelling flow directly beneath the margin of the cratonic lithosphere is also a characteristic component of edge-driven convection (*5–8*). These downwellings form beneath the margins of the thick cratonic lithosphere and have a similar magnitude thermal anomaly (although of opposite sign) to the upwellings. Evidence for downwelling flow associated with edge-driven convection is now available through the recently derived seismic tomographic model, S20RTS (Fig. 3) (*17*). At 350 km depth, model S20RTS yields an elongated, 1 to 2% high-velocity anomaly beneath the Atlantic coast of Africa and, albeit with a lower amplitude, a high-velocity anomaly in the transition zone, located beneath eastern Brazil and the central Atlantic Ocean. These anomalies are nearly equally as strong as high-velocity anomalies seen in S20RTS beneath subduction zone regions (e.g., South America and the western Pacific). High shear velocity anomalies are located at the eastern and western flanks of the South American and African cratons, respectively, and they extend to about 600 km depth (Fig. 3). Resolution tests indicate that the depth extent of shear velocity anomalies in the transition zone is poorly resolved. However, we can rule out the possibility that, due to incomplete data coverage, high-velocity structures in the uppermost 200 km of the mantle beneath cratons have been projected into the transition zone [Web fig. 1 (*18*)]. Because subduction beneath Africa has not occurred since the Triassic, we infer that the high-velocity structure reflects mantle downwellings beneath the western margin of the West African, Congo, and Kaapvaal cratons associated with edge-driven convection. The magnitude of the high shear velocity anomalies are consistent with the magnitude of the cold thermal anomalies in the numerical models (about 200°C) (*19*).

It is intriguing that in the North Atlantic, the youngest and narrowest part of the Atlantic basin, hot spots occur on the ridge axis (Iceland and Azores), while in the Central and Southern Atlantic there are a significant number of off-ridge hot spots (Bermuda, Madeira, Canary Islands, Cape Verde, Fernando, Arnold Seamount, Trindad, Mount Cameroon, and Vema). This is also consistent with the predictions of edge-driven convection. S20RTS (*17*) also indicates the presence of a high-velocity anomaly in the 300 km depth range beneath the eastern United States, which may be related to the Bermuda hot spot. Although this anomaly is significantly weaker than the African anomaly, it suggests that edge-driven convection may be responsible for other hot spots as well.

References and Notes

1. A. A. Nyblade, H. N. Pollack, *J. Geophys. Res.* 98, 12207 (1993); H. N. Pollack, S. J. Hurter, J. R. Johnson, *Rev. Geophys.* 31, 267 (1993).
2. J. D. Kramers, *Earth Planet. Sci. Lett.* 42, 58 (1979); S. H. Richardson, J. J. Gurney, A. J. Erlank, J. W. Harris, *Nature* 310, 198 (1984); F. R. Boyd, J. J. Gurney, S. H. Richardson, *Nature* 315, 387 (1985); S. H. Richardson, J. W. Harris, *Earth Planet. Sci. Lett.* 151, 271 (1997).
3. T. H. Jordan, *Nature* 274, 544 (1978); A. L. Lerner Lam, T. H. Jordan, *J. Geophys. Res.* 92, 14007 (1987); D. L. Anderson, J. Perlt, *Geology* 23, 205 (1995).
4. S. van der Lee, G. Nolet, *J. Geophys. Res.* 102, 22815 (1997); G. Ekström, A. M. Dziewonski, *Nature* 394, 168 (1998); J. Ritsema, H. van Heijst, *Geology* 28, 63 (2000).
5. S. D. King, D. L. Anderson, *Earth Planet. Sci. Lett.* 136, 269 (1995); S. D. King, D. L. Anderson, *Earth Planet. Sci. Lett.* 160, 289 (1998); C. E. Keen, R. R. Boutilier, in *Rifted Ocean-Continent Boundaries*, E. Banda *et al.*, Eds. (Kluwer, Dordrecht, Netherlands, 1995), pp. 17–30.
6. J. Elder, *The Bowels of the Earth* (Oxford Univ. Press, Oxford, 1976).
7. P. R. Vogt, *Geology* 19, 41 (1991).
8. J. C. Mutter, W. R. Buck, C. M. Zehnder, *J. Geophys. Res.* 93, 1031 (1988); W. S. Holbrook, B. Kelemen, *Nature* 364, 433 (1993).
9. D. L. Anderson, in *The Core Mantle Boundary Region*, vol. 28 of AGU Geodynamics Series, M. Gurnis, M. E. Wysession, E. Knittle, B. A. Buffett, Eds. (American Geophysical Union, Washington, DC, 1998), pp. 255–271.
10. S. D. King *et al.*, *Phys. Earth Planet. Inter.* 59, 195 (1990); J. J. Ita, S. D. King, *J. Geophys. Res.* 99, 15919 (1994). The calculations are in a 2890 by 2890 km domain with 256 bilinear elements in each direction. The Rayleigh number is 2.5×10^7, a reasonable approximation for Earth. The model parameters are chosen so that the resulting surface heat flow approximates the mean surface heat flow of Earth.
11. The solution for the thermal evolution of a cooling half-space has the form,
$$\theta(z) = \theta_0 \mathrm{erf}\left[\frac{-z}{2\sqrt{\kappa t}}\right]$$
where θ is temperature, t is time, κ is thermal diffusivity, z is the depth, and θ_0 encompasses the initial conditions. In the plate solution, time is related to the distance from the spreading axis, x, by the relation $x = v_{plate} \times t$, where v_{plate} is the plate velocity [A. R. Leeds, L. Knopoff, E. G. Kausel, *Science* 186, 141 (1974)].
12. The Clapeyron slopes used for these phase changes are 3.5 K/MPa (at 410 km) and −2.8 K/MPa (at 700 km). These are consistent with the values of the olivine to beta-spinel phase transformation (at about 410 km) and the ringwoodite to perovskite + magnesiowüstite phase transformation (at about 660 km) [C. Bina, G. Helffrich, *J. Geophys. Res.* 99, 15853 (1994)].
13. It is important to recognize that an organized downwelling slab from the thermal boundary layer would penetrate into the lower mantle with these model parameters while the smaller-scale, edge-driven flow remains confined to the upper mantle. This is consistent with previous studies of convection with phase changes which show that short-wavelength flows will not penetrate a phase boundary as easily as long-wavelength flows [P. J. Tackley, *Geophys. Res. Lett.* 23, 1985 (1996)].
14. S. Karato, P. Wu, *Science* 260, 771 (1993). There is an additional increase by a factor of 30 in viscosity at 700 km depth. This is consistent with many geophysical estimates of mantle rheology [B. H. Hager, M. A. Richards, *Philos. Trans. R. Soc. London A* 328, 309 (1989); S. D. King, *Rev. Geophys. (Suppl.)* 34, 11 (1995); A. M. Forte, J. X. Mitrovica, *Geophys. Res. Lett.* 23, 1147 (1996); J. X. Mitrovica, *J. Geophys. Res.* 101, 555 (1996)].
15. S. S. Shapiro, B. H. Hager, T. H. Jordan, *Lithos* 48, 115 (1999)]. The ±50 degree variations in temperature plotted in Fig. 2 represent a fraction of the thermal anomaly of the craton. The downwelling in Fig. 2 is composed almost entirely of cold mantle that has cooled at the edge of the craton and little cratonic material. Thus, the craton is not significantly eroded over the 100-My period in this calculation.
16. K. Burke, J. T. Wilson, *Nature* 239, 387 (1972); R. Thiessen, K. Burke, W. S. F. Kidd, *Geology* 7, 263 (1979).
17. J. Ritsema, H. J. van Heijst, J. H. Woodhouse, *Science* 286, 1925 (1999); J. Ritsema, H. J. van Heijst, *Sci. Prog.*, in press. Model S20RTS is a degree-20 shear velocity model of the mantle based on fundamental and higher mode Rayleigh wave phase velocities [H. J. Van Heijst, J. H. Woodhouse, *Geophys. J. Int.* 131, 209 (1997); *Geophys. J. Int.* 137, 601 (1999)] normal

mode splitting data [J. S. Resovsky, M. H. Ritzwoller, *J. Geophys. Res.* 104, 993 (1999)] and body wave travel times [J. Ritsema, H. J. Van Heijst, J. H. Woodhouse, *Eos* (*Spring Suppl.*) 80, S221 (1999)].

18. Supplementary Web figure is available at www.sciencemag.org/feature/data/1054178.shl
19. In a uniform composition mantle, in the absence of melting, we can write,

$$\delta T \approx \frac{(\delta V_s/V_s)}{(\partial \ln V_s/\partial \ln T)_p}$$

where T is temperature and V_s is the seismic shear velocity. Ignoring anelastic contributions to the velocity, which are probably small for cold anomalies in the upper mantle,

$$\delta T \approx \frac{-(\partial \ln \rho/\partial \ln V_s)_p}{\alpha} (\delta V_s/V_s)$$

where ρ is density and α is the coefficient of thermal expansion. Choosing reasonable upper mantle values for α and $(\partial \ln \rho/\partial \ln V_s)_p$, $\delta T \approx -1.0 \times 10^3\, \delta V_s/V_s$, which for a 2% velocity anomaly corresponds to 200 degrees.

20. N. L. Sleep, *Annu. Rev. Earth Planet. Sci.* 20, 19 (1992).

21. This research is funded by NSF. S.D.K. acknowledges support from NSF grants EAR-9726013 and EAR-9903002. This report is contribution number 8716 of the Division of Geological and Planetary Sciences, California Institute of Technology.

19 July 2000; accepted 11 October 2000